Progress In Electromagnetics Research, PIER 19, 173–197, 1998

SCATTERING FROM PERFECTLY CONDUCTING STRIPS BY UTILIZING AN ADAPTIVE MULTISCALE MOMENT METHOD

C. Su

Dept. of Applied Math.
Northwestern Polytechnical Univ.
Xian, Shaanxi, P.R. China

T. K. Sarkar

Dept. of ECE, Syracuse University
Syracuse, NY 13244-1240, USA

1. INTRODUCTION

Many numerical techniques have been proposed for the solution of electromagnetic scattering from large complex bodies. These method can be divided into two categories. One category is the hybrid technique which is the combination of high frequency methods and low-frequency method based on the physical characteristics of the bodies. Other is the computational technique based on mathematical subtleties, rather than on the physical characteristics of the bodies derived from eletromagnetics. For the hybrid techniques, many methods have been suggested. An approach of a hybrid analysis is that it

combines the high-frequency method with the moment method, such as a GTD-MM approach or a PTD-MM approach. In addition, there are current-based hybrid methods. A GTD-MM approach has been described in [1–4]. Examples of these methods can be found in these references. The current-based hybrid technique combines the MM technique with Ansatz surface currents obtained from the PO approximation, PTD,GTD and the Fock theory. According to the physical characteristics of the induced currents on the surface of the bodies, the whole boundary surface of the scatterer has been subdivided into irregular and smooth surfaces. The current on the smooth surfaces can be separated into a PO term plus a surface wave term resulting from the surface-wave effects. The current on the irregular surface and the surface-wave term can be solved for using the MM technique. The details of this technique and examples can be seen in [5–7]. Furthermore, Jakobus and Landstorfer [8, 9] suggested an improved PO-MM hybrid formulation for solution of scattering from three-dimensional perfectly conducting bodies of arbitrary shape. Another variation of the first category is the techniques that combines the high-frequency method with the finite element method or finite difference in time domain. Jin et al [10], used the high-frequency method known as Shooting-Bouncing-Ray method [11–13] and FEM [14–16] to evaluate the electromagnetic scattering by large bodies with cracks and cavities on their surfaces. The general coupling scheme has been developed to couple the interior and exterior fields in such a manner that it included all significant interactions and it permits the SBR and FEM to be computed separately. Lee and Chia [17] proposed a hybrid Ray-FDTD method for the analysis of electromagnetic scattering from a cavity with a complex termination. A high-frequency method, GRE [18] (generalized ray method) has been used to track the fields from the mouth of the cavity up to an arbitrarily defined planar surface close to the termination. The FDTD method is applied to the small region surrounding the termination.

The solution technique based on mathematical principles in computational electromagnetics are the two techniques of the multilevel or the multigrid method and the wavelet method.

The multilevel or multigrid method has been used widely in solving differential equations and integral equations in the area of computational mathematics. The multilevel method can be used to solve the EM scattering problem. A multilevel algorithm utilizing the moment

method has been developed by Kalbasi and Demarest [19]. The powerful multilevel algorithm for penetrable, volumetric scatterers have been developed by Lin and Chew [20] and Chew and Lu [21]. Another multilevel algorithm named as MLMDA (Multilevel Matrix Decomposition Algorithm) was first presented in [22] and has further been developed by Michielssen and Boag [23, 24] for analyzing scattering from electrically large surfaces. The other technique for solution of integral equations is the method of moments with wavelet basis or wavlet-like basis. Beylkin et al. [25] first proposed to solve the integral equation by use of wavelets. Alpert el al. [26] introduced wavelet-like basis function in solving second-kind integral equation. The wavelet basis or the wavelet-like basis have been chosen as basis functions in the MM of the integral equations of electromagnetic fields [see references [27–31]. Goswami et al. [32] proposed the use of compactly supported semi-orthogonal spline wavelets constructed for analyzing the two-dimensional electromagnetic scattering problems of metallic cylinders. Wang [33] proposed the hybrid wavelet expansion and boundary element method (HWBM) to solve the two-dimensional electromagnetic scattering problems over curved computation domain. In HWBM method, the unknown surface current was presented in terms of a basis of periodic, orthogonal wavelet in interval [0,1]. By the use of the wavelet basis or wavelet-like basis in the method of moments, the system matrix can be transformed into a sparse matrix due to their basis function having the local support and vanishing moment properties. Hence, it can reduce memory requirements and save CPU-time for the solution of electromagnetic field problems.

The induced current on the surface of the scatterer varies greatly in different regions. The classical way to deal with it, is to choose basis functions on a non-uniform grid. One can divide the whole domain into several different domains. In the different domains, different basis functions are chosen. But, it is difficult to subdivide the whole region if the solution is not known a priori.

The aim of this paper is to introduce the adaptive method for analysis of scattering from PC strip from the point of view of reducing the number of unknowns based on wavelet-like basis. This paper is organized as follows. Section 2 outlines the conventional moment method to analysis scattering problems of PC strip. Section 3 presents a new kind of basis functions on the multiscale and a new method for approximating a function based on the multiscale and wavelet-like basis.

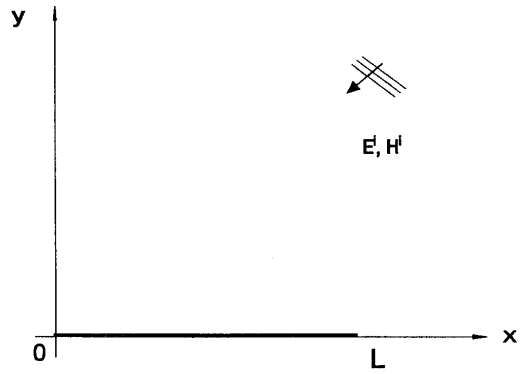

Figure 1. Geometry of scattering from a PC strip.

Section 4 presents the adaptive multiscale moment method to solve the EM integral equation. Section 5 describes numerical results obtained using the new technique for the PC strip. Finally, Section 6 outlines conclusions.

2. FORMULATION OF THE PROBLEM

The scattering analysis of flat PC strip (see Fig. 1) is expressed by an EFIE as

$$\vec{E}(\vec{r}) = \vec{E}^i(\vec{r}) - L[\vec{J}(\vec{r}')] \tag{1}$$

where the electric field $\vec{E}(\vec{r})$ at a field point $\vec{r} = (x, y)$ is expressed by the electric current density $\vec{J}(\vec{r})$ on the strip and $\vec{E}^i(\vec{r})$ is the incident electric field. The surface integral operator $L[\vec{J}(\vec{r}')]$ on the strip is defined as

$$L[\vec{J}(\vec{r}')] = L[J(x')] = \frac{\eta_0 k}{4}\left[\int_0^L J(x')H_0^{(2)}(k|x-x'|)dx' + \frac{1}{k^2}\frac{\partial}{\partial x}\int_0^L \frac{dJ(x')}{dx'}H_0^{(2)}(k|x-x'|)dx'\right] \quad \text{for TE case}$$

$$L[\vec{J}(\vec{r}')] = L[J(x')] = \frac{\eta_0 k}{4}\left[\int_0^L J(x')H_0^{(2)}(k|x-x'|)dx'\right]$$

for TM case

where $\eta_0 = \sqrt{u_0/\varepsilon_0} \approx 377\Omega$.

The incident electric field $\vec{E}^i(\vec{r})$ on the strip can be chosen in the following form

$$E^i_{strip}(x) = \begin{cases} E_0 e^{jkx\cos\varphi_i}\sin\varphi_i & \text{for TE case;} \\ E_0 e^{jkx\cos\varphi_i} & \text{for TM case.} \end{cases} \tag{2}$$

Hence, the scale integral equation can be obstained

$$g(x) = L[J(x')] \tag{3}$$

where $g(x) = E^i_{strip}(x)$

In the above integral equation, the induced surface current density $J(x')$ is the only unknown, and can be determined by the conventional moment method. Suppose the unknown current density $J(x')$ on PC strip is approximated by a finite set $u_n(x)$ of basis functions, that is

$$J(x') = \sum_{n=1}^{N} a_n u_n(x') \tag{4}$$

where N is the number of basis functions needed to cover the PC strip and the expansion coefficients a_n are to be determined. In the conventional moment method, the basis functions used in solving radiating or scattering problems are chosen as the subdomain functions, such as pulse functions, triangular functions and piecewise sinusoidal functions. Substituting the approximate representation of the induced current density $J(x')$ into the equation (3), we obtain

$$g(x) = \sum_{n=1}^{N} a_n L[u_n(x')] \tag{5}$$

In order to solve the unknowns a_n, by multiply the above equation by weight functions $w_n(x)$ (which can be selected the same as the

basis functions $u_n(x)$) and integrating over the strip region, a set of N simultaneous equations is obtained

$$g_m = \langle g(x), u_m(x) \rangle = \sum_{n=1}^{N} a_n \langle L\left[u_n(x')\right], u_m(x) \rangle \; m = 1, 2, ..., N \quad (6)$$

Written in matrix form as

$$ZI = V \quad (7)$$

where $I = (a_1, a_2, ..., a_N)^T$, $Z = \{\langle L\left[u_n(x')\right], U_m(x)\rangle\}_{(N\times N)}$, $V = (g_1, g_2, ..., g_N)^T$.

Once I is determined by use of solving the linear equations, the induced current density can be determined from (4). The scattering cross section $\sigma(\varphi, \varphi_i)$ can be obtained by

$$\sigma(\varphi, \varphi_i) = \begin{cases} \dfrac{k\eta_0^2}{4}\left|\displaystyle\int_0^L J(x) e^{jkx\cos\varphi} dx\right|^2 & \text{for TM;} \\ \dfrac{k}{4}\left|\displaystyle\int_0^L J(x) e^{jkx\cos\varphi} \sin\varphi dx\right|^2 & \text{for TE.} \end{cases} \quad (8)$$

where φ is the angle at the observation point.

The conventional moment method requires approximately ten unknowns per wavelength and is difficult to be applied to analysis the large scatterers. For the present method, we seek to maximize the reduction of unknowns by the development of an efficient representation of the unknown current density based on wavelet-like basis. In the next section, we introduce a new kind of basis based on multiscale (similar to multigrid), and the unknown current density is approximated by the linear combination of the wavelet-like basis.

3. A NEW KIND OF BASIS FUNCTIONS ON THE MULTISCALE

The triangular basis functions of uniform grid on the interval $[0, L]$ with $N + 1$ nodes can be given by

$$\begin{aligned} \phi_0(x) &= \phi_{0,1}(x) \\ \phi_N(x) &= \phi_{0,2}(x - L) \end{aligned} \quad (9)$$

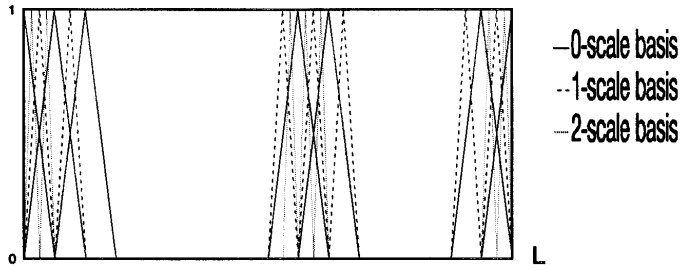

Figure 2. Geometry of bais functions on 0-scale,1-scale and 3-scale.

$$\phi_i(x) = \phi_{0,1}(x - x_{0,1}) + \phi_{0,2}(x - x_{0,i}) \quad i = 1, 2, ..., N-1$$

where $x_{0,i} = \frac{iL}{N} = ih, i = 0, 1, 2, ..., N, h = \frac{L}{N}$

$$\phi_{0,1}(x) = \begin{cases} 1 - \frac{N}{L}x & [0, h] \\ 0 & \text{other} \end{cases}$$

$$\phi_{0,2}(x) = \begin{cases} 1 + \frac{N}{L}x & [-h, 0] \\ 0 & \text{other} \end{cases}$$

The function $g(x)$ on $[0, L]$ can be approximated by these triangular basis functions, that is

$$g(x) \approx g_0(x) = \sum_{n=0}^{N} g(x_{0,n})\phi_n(x) \tag{10}$$

Through multiscale in the interval $[0, L]$, the new nodes are located at

$$x_{1,i} = \frac{x_{0,i-1} + x_{0,i}}{2} = (i - \frac{1}{2})h$$

and the new basis functions (shown in Fig. 2) are

$$\phi_{1,i} = \phi_{0,1}[2(x - x_{1,i})] + \phi_{0,2}[2(x - x_{1,i})] \tag{11}$$

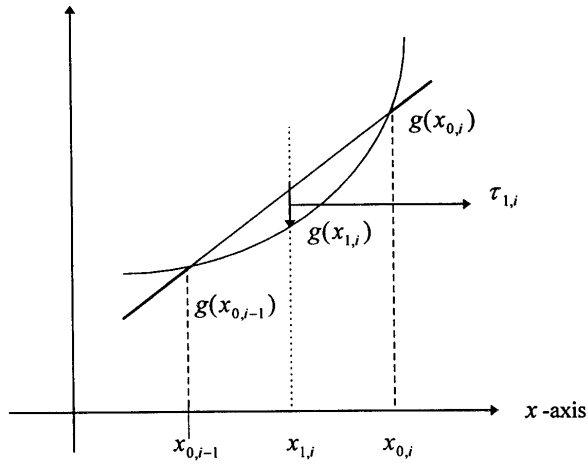

Figure 3. Geometry of coefficient $\tau_{1,i}$.

After the first multiscale, the approximate function $g_1(x)$ is represented as follows:

$$g_1(x) = g_0(x) + \sum_{i=1}^{N} \tau_{1,i}\phi_{1,i}(x) \tag{12}$$

where $\tau_{1,i}$ are unknown coefficients. Suppose $g_1(x_{1,i}) = g(x_{1,i})$, then:

$$\tau_{1,i} = g(x_{1,i}) - g_0(x_{1,i}) = g(x_{1,i}) - \frac{1}{2}(g(x_{0,i-1}) + g(x_{0,i})) \tag{13}$$

If $g(x)$ possesses the two-order continuous differentiability condition on $[0, L]$, the following approximate formula leads

$$\tau_{1,i} \approx -\frac{h^2}{4} g''(x_{1,i}) \tag{14}$$

Geometrically, $\tau_{1,i}$ means the difference between the linear approximate function on $[0, L]$ and the original function $g(x)$ at the middle point $x_{1,i}$ (see Fig. 3). Therefore, if $g(x)$ is a linear function on some local interval in $[0, L]$, some coefficients $\tau_{1,i}$ will be zero. We can repeat the same procedure on the interval $[0, L]$ several times. Through

V-times multiscale the interval $[0, L]$ the newly formed nodes are

$$x_{V,i} = \left(\frac{1}{2^V} + \frac{i-1}{2^{V-1}}\right) h, \quad i = 1, 2, ..., 2^{V-1}N \tag{15}$$

and the newly formed basis functions are

$$\phi_{V,i}(x) = \phi_{0,1}[2^V(x - x_{V,i})] + \phi_{0,2}[2^V(x - x_{V,i})] \tag{16}$$

The V'th approximation function $g_V(x)$ is represented by

$$\begin{aligned} g_V(x) &= g_{V-1}(x) + \sum_{i=1}^{2^{V-1}N} \tau_{V,i}\phi_{V,i}(x) \\ &= \sum_{i=0}^{N} g(x_{0,i})\phi_n(x) + \sum_{j=1}^{V}\sum_{i=1}^{2^{J-1}N} \tau_{j,i}\phi_{j,i}(x) \end{aligned} \tag{17}$$

where $\tau_{j,i}$ are unknown coefficients. Let $g_V(x_{V,i}) = g(x_{V,i}), i = 1, 2, ..., 2^{V-1}N$, then

$$\begin{aligned} \tau_{V,i} &= g(x_{V,i}) - g_{V-1}(x_{V,i}) \\ &= g(x_{V,i}) - g_0(x_{V,i}) - \sum_{j=1}^{V}\sum_{n=1}^{2^{j-1}N} \tau_{j,n}\phi_{j,n}(x_{J,i}) \\ &= g(x_{V,i}) - \frac{1}{2}\left(g(x_{V,i} - \frac{1}{2^V}h) + g(x_{V,i} + \frac{1}{2^V}h)\right) \end{aligned}$$

If $g(x)$ possesses the two-order continuous differentiable at $x_{V,i}$, then

$$\tau_{V,i} \approx -\frac{h^2}{2^{V+2}}\left|g''(x_{V,i})\right| \tag{18}$$

If $|\tau|_{j,i} \leq \varepsilon$ (ε is the given threshold), $\tau_{j,i}$ is set to be zero. Then the maximum multiscale V can be estimated by the following formula

$$V \approx \log_2\left[\frac{h^2}{4\varepsilon}\max_{x\in[0,L]}\left|g''(x)\right|\right] \tag{19}$$

We can prove that the new kind of basis functions on V-times multiscale is equivalent to the triangular basis functions on the uniform grid with the nodes $\left\{X_m = mh; \quad m = 0, 1, 2, ..., 2^V N; \quad h = \frac{L}{2^V N}\right\}$.

In the next section, we choose this kind of basis to study the scattering problem of PC strip by the moment method.

4. ADAPTIVE MULTISCALE MOMENT METHOD

Suppose the electric current density is expressed by the multiscale basis functions

$$J(x) = \sum_{i=0}^{N} \tau_i \phi_i(x) + \sum_{v=1}^{V} \sum_{i=1}^{2^{v-1}N} \tau_{v,i} \phi_{v,i}(x) \tag{20}$$

where $\{\tau_i, \tau_{v,i}\}$ is the complex unknowns. Substituting (20) into (3), results in

$$g(x) = \sum_{i=0}^{N} \tau_i L[\phi_i(x')] + \sum_{v=1}^{V} \sum_{i=1}^{2^{v-1}N} \tau_{v,i} L[\phi_{v,i}(x')] \tag{21}$$

By utilizing Galerkin method where the testing functions are the same as the basis functions, we can obtain the set of linear equations:

$$\begin{aligned} \langle g(x), \phi_m(x) \rangle = & \sum_{i=0}^{N} \tau_i \langle L[\phi_i(x')], \phi_m(x) \rangle + \\ & \sum_{v=1}^{V} \sum_{i=1}^{2^{v-1}N} \tau_{v,i} \langle L[\phi_{v,i}(x')], \phi_m(x) \rangle \end{aligned}$$

$$\begin{aligned} \langle g(x), \phi_{v',i'}(x) \rangle = & \sum_{i=0}^{N} \tau_i \langle L[\phi_i(x')], \phi_{v',i'}(x) \rangle + \\ & \sum_{v=1}^{V} \sum_{i=1}^{2^{v-1}N} \tau_{v,i} \langle L[\phi_{v,i}(x')], \phi_{v',i'}(x) \rangle \end{aligned}$$

The set of equations can be written in matrix form as

$$\begin{pmatrix} F_0 \\ F_1 \\ \vdots \\ F_V \end{pmatrix} = \begin{pmatrix} A_{0,0} & A_{0,1} & \dots & A_{0,V} \\ A_{1,0} & A_{1,1} & \dots & A_{1,V} \\ \vdots & \vdots & \ddots & \vdots \\ A_{V,0} & A_{V,1} & \dots & A_{V,V} \end{pmatrix} \begin{pmatrix} X_0 \\ X_1 \\ \vdots \\ X_V \end{pmatrix} \tag{22}$$

where $X_0 = (\tau_0, \tau_1, ..., \tau_N)^T, X_v = (\tau_{v,1}, \tau_{v,2}, ..., \tau_{v,2^{v-1}N})^T, (v = 1, 2, ..., V)$

$$F_0(i) = \frac{4}{k\eta_0} \int_0^L g(x)\phi_m(x)dx$$

$$m = 0, 1, 2, ..., N$$

$$F_v(i) = \frac{4}{k\eta_0} \int_0^L g(x)\phi_{v,i}(x)dx$$

$$v = 1, 2, ..., V, i = 1, 2, ..., 2^{v-1}N$$

$$A_{0,0}(i, m) = \int_0^L \phi_i(x)L[\phi_m(x')]dx$$

$$i = 0, 1, 2, ..., N, m = 1, 2, ..., N$$

$$A_{0,J}(i, m) = \int_0^L \phi_i(x)L[\phi_{J,m}(x')]dx$$

$$i = 0, 1, 2, ..., N, m = 1, 2, ..., 2^{J-1}N$$

$$A_{J,0}(m, i) = \int_0^L \phi_{J,m}(x)L[\phi_i(x')]dx$$

$$i = 0, 1, 2, ..., N, m = 1, 2, ..., 2^{J-1}N$$

$$A_{J,V}(i, m) = \int_0^L \phi_{J,i}(x)L[\phi_{V,m}(x')]dx$$

$$i = 1, 2, ..., 2^{J-1}N, m = 1, 2, ..., 2^{V-1}N$$

The formula for $F_0(i)$, $F_v(i)$, $A_{0,0}(i, m)$, $A_{0,J}(i, m)$, $A_{J,0}(m, i)$, $A_{J,V}(i, m)$ depending on the TE and TM cases can easily be computed. Once the above linear equation is solved, the current density can be determined. The computation of the scattering cross section of the PC strip can be obtained from

$$\sigma(\varphi,\varphi_i)=\frac{k\eta_0^2}{4}\Bigg|\tau_0\frac{1}{jk\cos\varphi}\left[e^{\frac{jkh\cos\varphi}{2}}SINC\left(\frac{kh\cos\varphi}{2}\right)-1\right]+\tau_N\frac{e^{j}kL\cos\varphi}{jk\cos\varphi}\left[1-e^{\frac{jkh\cos\varphi}{2}}SINC\left(\frac{kh\cos\varphi}{2}\right)\right]+\sum_{i=1}^{N-1}\tau_i e^{jkx_{0,i}\cos\varphi}hSINC^2\left(\frac{kh\cos\varphi}{2}\right)\sum_{v=1}^{V}\sum_{i=1}^{2^{v-1}N}\tau_{v,i}e^{jkx_{v,i}\cos\varphi}\frac{h}{2^v}SINC^2\left(\frac{kh\cos\varphi}{2^{v+1}}\right)\Bigg|^2 \quad \text{for TM} \tag{23a}$$

$$\sigma(\varphi,\varphi_i)=\frac{k\sin^2\varphi}{4}\Bigg|\sum_{i=1}^{N-1}\tau_i e^{jkx_{0,i}\ cos\varphi}hSINC^2\left(\frac{kh\cos\varphi}{2}\right)+\sum_{v=1}^{V}\sum_{i=1}^{2^{v-1}N}\tau_{v,i}e^{jkx_{v,i}\cos\varphi}\frac{h}{2^v}SINC^2\left(\frac{kh\cos\varphi}{2^{v+1}}\right)\Bigg|^2 \quad \text{for TE} \tag{23b}$$

where $SINC(x)=\frac{sin(x)}{x}$. Now, we discuss how to solve the linear equation (22).

First, it can be found that the coefficient matrix and the left-hand term has important characteristics on different scales. From V-scale to $(V+1)$-scale, there may be increase in the number of elements in the coefficient matrix and the left-hand array. But some of elements of the coefficient matrix and the left-hand array do not change while increasing the scale. This is an essential distinction from the multigrid or multilevel technique of solving an integral equation. The illustration of how the coefficient matrix the left-hand array and the unknowns scale can be seen in Fig. 4.

Another important characteristics is that the solution $(X_0, X_1, ..., X_V)$ on V-scale is closely related to the solution $(X_0, X_1, ..., X_V, X_{V+1})$ on $(V+1)$-scale. As we know, the electric current density $J_V(x)$ on V-scale and J_{V+1} on $(V+1)$-scale has the following relation:

$$J_{v+1}(x)=J_V(x)+\sum_{i=1}^{2^V N}\tau_{V+1,i}\phi_{V+1,i}(x),$$

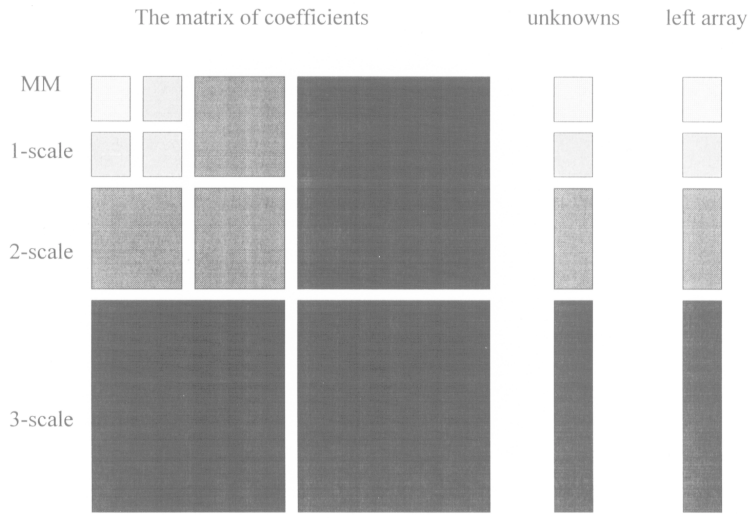

Figure 4. The illustration of the coefficient matrix,left array and the unknowns.

In general, the current density $J(x)$ has a two-order derivative on $[0, L]$. So there is a relation between $\tau_{V+1,i}$, and $J''(x)$ at the points $X_{V+1,i}$. Hence an approximate solution for the unknown array X_{V+1}, can be estimated through the obtained solutions $(X_0, X_1, ..., X_V)$ on V-scale by use of an interpolation method. The suitable initial guess on $(V+1)$-scale can be provided in order to solve the linear $J(x)$ is smooth or is a linear function in some local regions, then some $\tau_{v,i}$ will be approximately zero. For a given threshold ε and an initial guess $\{\tau_{v,i}\}(v = 1, 2, ..., V; i = 1, 2, ..., 2^{v-1}N)$ we set the following $\tau_{v,i}$ to zero, if $|\tau_{v,i}| < \varepsilon$. We omit the elements of the arrays, the columns of the coefficient matrix and the elements of the left-hand array corresponding to the term $\tau_{v,i} = 0$ and form the new set of equations which are solved by the CG method. Because the order of the original equation is reduced by eliminating the rows and columns corresponding to the unknowns that are eliminated, it will improve the computational efficiency. The computational flow chart of the adaptive multiscale moment method from V-scale to $(V+1)$-scale is given in Fig. 5.

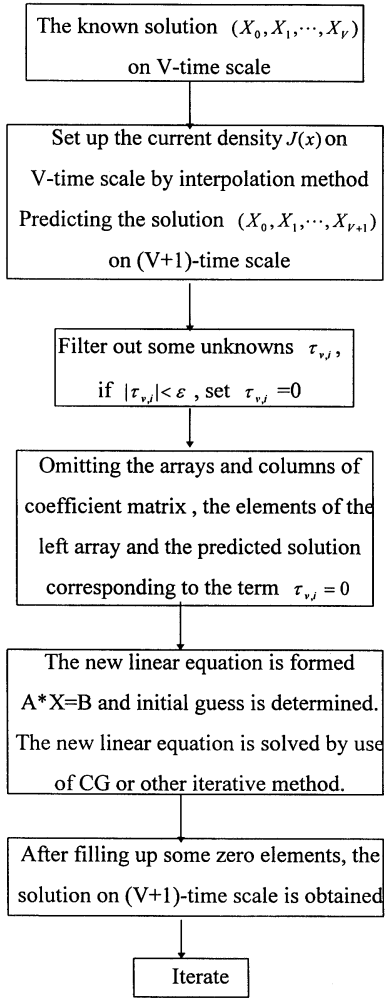

Figure 5. Flow chart of the adaptive multiscale moment method.

5. NUMERICAL RESULTS

This section provides some numerical results obtained by the use of the adaptive multiscale moment method for analysis of TE or TM scattering from perfectly conducting strips. For simplicity, in the numerical interpolation for estimating the coefficients, we choose the following method. For the points in the middle of the region, suppose the known data is $\{f(-\frac{3}{2}h), f(-\frac{1}{2}h), f(\frac{1}{2}h), f(\frac{3}{2}h)\}$ can be computed

from the following formula by using a cubic polynomial approximation as

$$f(0) = \frac{\left[f(-\frac{1}{2}h) + f(\frac{1}{2}h)\right] - \left[f(-\frac{3}{2}h) + f(\frac{3}{2}h)\right]}{6}$$

For the point to the left of the region of the known data $\{f(-\frac{1}{2}h), f(\frac{1}{2}h), f(\frac{3}{2}h)\}$, the value $f(0)$ can be computed using the quadratic polynomial approximation

$$f(0) = \frac{\left[f(-\frac{1}{2}h) + f(\frac{1}{2}h)\right]}{2} - \frac{\left[2f(-\frac{1}{2}h) + f(\frac{3}{2}h)\right]}{3}$$

For the point to the right of the region of the known data $\{f(-\frac{3}{2}h), f(-\frac{1}{2}h), f(\frac{1}{2}h)\}$, the value $f(0)$ can be computed from the quadratic polynomial approximation

$$f(0) = \frac{\left[f(-\frac{1}{2}h) + f(\frac{1}{2}h)\right]}{2} - \frac{\left[2f(\frac{1}{2}h) + f(-\frac{3}{2}h)\right]}{3}$$

So interpolation can be used to estimate the coefficients.

As a first example, consider a flat PC strip of 1λ for TM excitation. In this case, the size of the linear equation of the adaptive multiscale moment method with different thresholds and incident angles are listed in Table 1–3. The number of the initial division N on the 1λ strip is taken as 8.

It is seen from the tables that the size of the moment matrix can be significantly be reduced from 257 by utilizing different scales V and by setting different thresholds ε to set the unknowns equal to zero by observing $\tau_{v,i}$. Setting a larger threshold ε for the amplitude of the unknown expansions a smaller matrix is obtained. The case $\varepsilon = 0$ would be the standard MOM. The results for the RCS are quite in sensitive to the various scales even though the currents display some irreguralities for low scale values.

The magnitude and the phase of the current density and the bistatic RCS for the case of the incident angle $\phi = 45^\circ$ and $\varepsilon = 0.01$ is plotted in Fig. 6.

Next consider scattering from the flat PC strip of 4.5λ length for the TE case. The order of the linear equation of the adaptive multiscale moment method for different thresholds and incident angles are listed in Table 4 and 5. The number of initial division N is taken as 8.

Again for this case it is seen that by utilizing this adaptive multiscale moment method it is possible to significantly reduce the number

N=8	ε=0	ε=0.001	ε=0.01	ε=0.1
V=0	9	9	9	9
V=1	17	17	17	13
V=2	33	31	17	15
V=3	65	43	20	16
V=4	129	56	21	16
V=5	257	83	23	17

Table 1. Normal Incidence .

N=8	ε=0	ε=0.001	ε=0.01	ε=0.1
V=0	9	9	9	9
V=1	17	17	17	11
V=2	33	33	17	12
V=3	65	61	20	12
V=4	129	75	20	14
V=5	257	88	22	14

Table 2. (Incident angle $\phi = 10^\circ$).

N=8	ε=0	ε=0.001	ε=0.01	ε=0.1
V=0	9	9	9	9
V=1	17	17	16	11
V=2	33	32	17	12
V=3	65	52	20	12
V=4	129	57	21	14
V=5	257	70	23	13

Table 3. (Incident angle $\phi = 45^\circ$).

N=8	ε=0	ε=0.01	ε=0.04	ε=0.1
V=0	7	7	7	7
V=1	15	15	13	11
V=2	31	29	25	21
V=3	63	59	44	23
V=4	127	101	33	20
V=5	255	203	38	19

Table 4. Normal incidence.

N=8	ε=0	ε=0.01	ε=0.04	ε=0.1
V=0	7	7	7	7
V=1	15	15	15	15
V=2	31	31	29	28
V=3	63	63	56	38
V=4	127	123	70	28
V=5	255	221	84	28

Table 5. (Incident angle $\phi = 45°$.)

of unknowns from 255 by applying the threshold to the extrapolated values for the unknowns. Again, $\varepsilon = 0$ corresponds to the standard MOM results. The magnitude and the phase of the current density and the bistatic RCS for the case of the incident angle $\phi = 45°$ and $\varepsilon = 0.04$ is plotted in Fig. 7.

For the third example, consider scattering from the flat PC strip of 10λ with TM illumination. The size of the linear equations of the adaptive multiscale moment method for different thresholds and incident angles are listed in Table 6 and 7. The number of initial discretization point N is taken as 8.

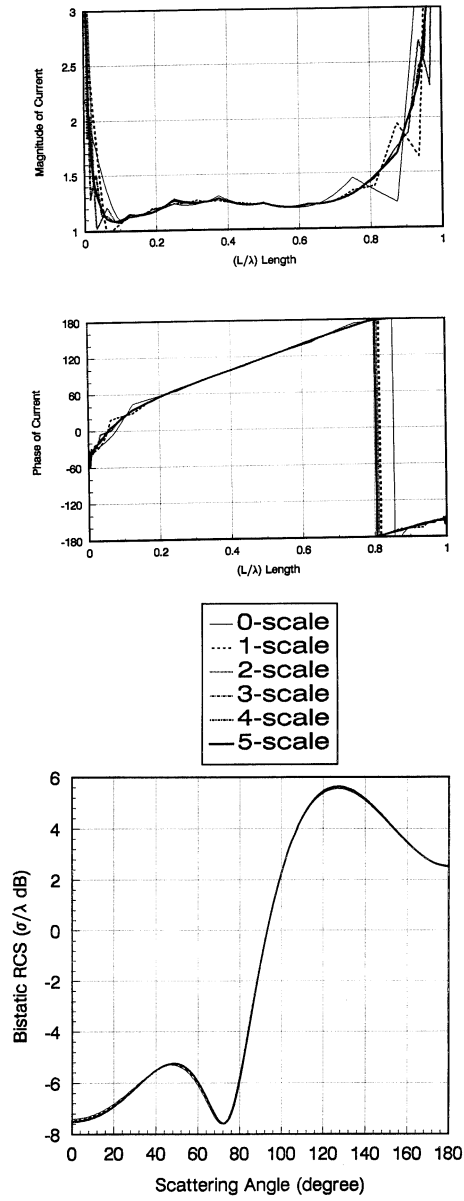

Figure 6. Strip's Length $L = \lambda$, incident angle $\theta = 45°$, initial divided nodes $N = 8$, maximum scale $V = 5$ threshold $\varepsilon = 0.01$ TM case.

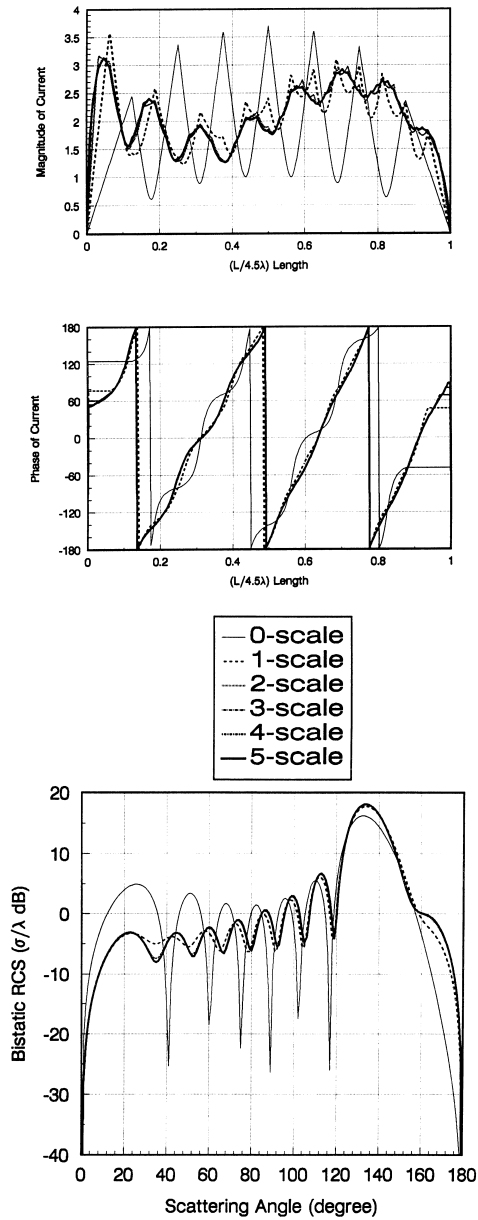

Figure 7. Strip's Length $L = 4.5\lambda$, incident angle $\theta = 45°$, initial divided nodes $N = 8$, maximum scale $V = 5$ threshold $\varepsilon = 0.04$ TE case.

N=8	ε=0	ε=0.001	ε=0.01	ε=0.1
V=0	9	9	9	9
V=1	17	17	13	9*
V=2	33	31	20	9*
V=3	65	51	24	9*
V=4	129	68	25	9*
V=5	257	79	28	9*

Table 6. Normal incidence.

N=8	ε=0	ε=0.01	ε=0.04	ε=0.1
V=0	9	9	9	9
V=1	17	17	15	13*
V=2	33	33	28	19*
V=3	65	65	57	30*
V=4	129	129	92	28*
V=5	257	160	90	29*

Table 7. (Incident angle $\phi = 45°$).

In the above table, * means that the results is not correct due to too few unknowns.

The magnitude and the phase of the current density and the bistatic RCS for the case of the normal incidence and $\varepsilon = 0.01$ is plotted in Fig. 8 . From Tables 4, 5, and 7, it is seen that the adaptive multiscale moment method require more unknowns when the incident angle is away from the normal. The reason is that the phase of the induced current density varies with a certain period on the whole strip for non broadside illumination. However, the total number of unknowns can still be lower than the standard MOM.

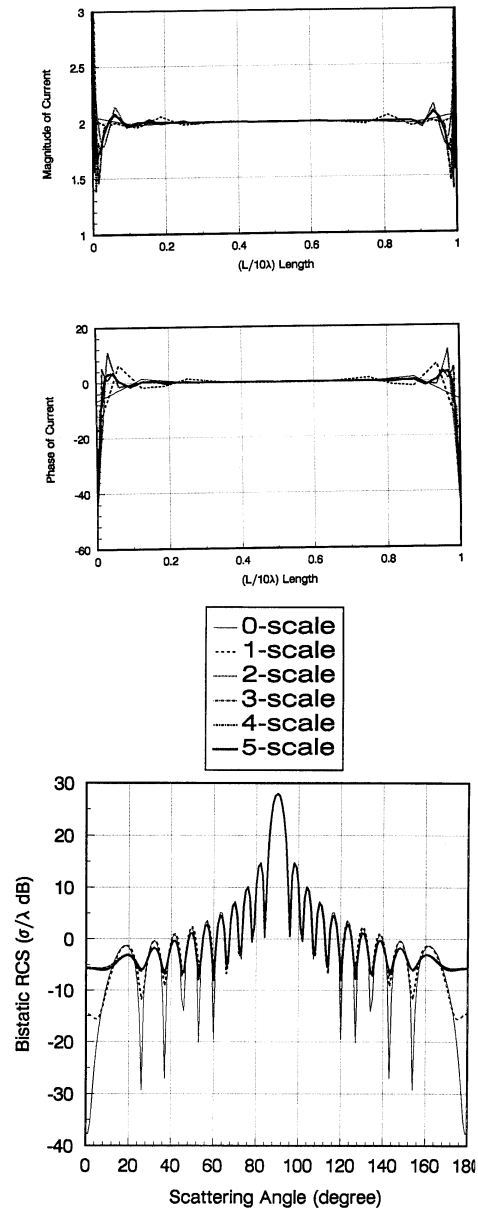

Figure 8. Strip's Length $L = 10\lambda$, incident angle $\theta = 90°$, initial divided nodes $N = 8$, maximum scale $V = 5$ threshold $\varepsilon = 0.01$ TM case.

6.CONCLUSION

The adaptive multiscale moment method has been presented as an approximation method utilizing the wavelet-like basis, where the electric current density is expressed by a linear combinations of wavelet-like basis functions on different scales. According to the characteristics of the approximate expression of the current density and because of the local supports of the wavelet-like basis, the unknowns on $(V+1)$-scale can be estimated from the computed solution on V-scale. Since some of the unknowns which are relatively small can be filtered out. The number of unknowns are less than the standard MOM solution providing similar accuracy of the solution. Therefore, this method leads to a reduction of the computation time and storage memory. The results obtained from the adaptive multiscale moment method are in close agreement with those solved by the conventional moment method as described in [5]. Although we have studied the scattering problems of PC strip, the approach can be extended to curved surface. The extension of this technique to other two and three dimensions is currently underway.

REFERENCES

1. Thiele, G. A., and T. H. Newhouse, "A hybrid technique for combining moment methods with a geometrical theory of diffraction," *IEEE Trans. Antennas Propagat.*, Vol. AP-23, 62–69, Jan. 1975.
2. Burnside, W. D., C. L. Lu, and R. J. Marhefka, "A technique to combine the geometric theory of diffraction and the moment method," *IEEE Trans. Antennas Propagat.*, Vol. AP-23, 551–558, May 1975.
3. Ekelman, E. P., and G. A. Thiele, "A hybrid technique for combining the moment method treatment of wire antennas with the GTD for curved surfaces," *IEEE Trans. Antennas Propagat.*, Vol. AP-28, 831–839, June 1980.
4. Sahalos, J. N., and G. A. Thiele, "On the application of the GTD-MM technique and its limitation," *IEEE Trans. Antennas Propagat.*, Vol. AP-29, 780–786, June 1981.
5. Medgyesi-Mitschang, L. N., and D. S. Wang, "Hybrid solutions for scattering from perfectly conducting bodies of revolution," *IEEE Trans. Antennas Propagat.*, Vol. AP-31, 570–583, May 1983.
6. Medgyesi-Mitschang, L. N., and D. S. Wang, "Hybrid solutions for scattering from large bodies of revolutlon with material dis-

continuities and coatings," *IEEE Trans. Antennas Propagat.*, Vol. AP-32, 717–723, June 1984.
7. Wang, D. S., "Current-basesd hybrid analysis for surface-wave effects on large scatterers," *IEEE Trans. Antennas Propagat.*, Vol. AP-39, 839–850, June 1991.
8. Jakobus, U., and F. M. Landstorfer, "Improved PO-MM hybrid formulation for scattering from three-dimensional perfectly conducting bodies of arbitrary shape," *IEEE Trans. Antennas Propagat.*, Vol. AP-43, 162–169, Feb. 1995.
9. Jakobus, U., and F. M. Landstorfer, "Improvement of the PO-MoM hybrid method by accounting for effects of perfectly conducting wedges," *lEEE Trans. Antennas Propagat.*, Vol. AP-43, 1123–1129, Oct. 1995.
10. Jin, J., S. S. Ni, and S. W. Lee, "Hybridization of SBR and FEM for scattering by large bodies with cracks and cavities," *IEEE Trans. Antennas Propagat.*, Vol. AP-43, 1130–1139, Oct. 1995.
11. Ling, H., R. C. Chou, and S. W. Lee, "Ray Versus modes: Pictorial display of energy flow in an open-ended waveguided," *IEEE Trans. Antennas Propagat.*, Vol. AP-35, No. 3, 605–607, May, 1987.
12. Ling, H., R. C. Chou, and S. W. Lee, "Shooting and Bouncing Ray: calculatin the RCS of an arbitrary shaped cavity ," *IEEE Trans. Antennas Propagat.*, Vol. AP-37, No. 2, 194–205, Feb. 1989.
13. Baldauf, J., S. W. Lee, L. Lin, S. K. Jeng, S. M. Scarborouh, and C. L. Yu, "High frequency scattering from trihedral corner reflectors and other benchmark targets: SBR versus experiments," *IEEE Trans. Antennas Propagat.*, Vol. AP-39, No. 9, 1345–1351, Sept. 1991.
14. Jin, J. M., and J. L. Volakis, " A finite element boundary integral formulation for scattering by three-dimensional cavity-backed apertures," *IEEE Trans. Antennas Propagat.*, Vol. AP-39, No. 1, 97–104, 1991.
15. Jin, J. M, and J. L. Volakis, " A hybrid finite element method for scattering and radiation by microstrip patch antennas and arrays residing in a cavity," *IEEE Trans. Antennas Propagat.*, Vol. AP-39, No. 11 1598–1604, Nov. 1991.
16. Jin, J. M., "The finite element method in electromagnetics", New York, Wiley, 1993.
17. Lee, R., and T. T. Chia, "Analysis of electromagnetic scattering from a cavity with a complex termination by means of a hybrid Ray-FDTD method," *IEEE Trans. Antennas Propagat.*, Vol. AP-41, No. 11, 1560–1564, Nov. 1993.

18. Burkholder, R. J., "High-frequency asymptotic methods for analyzing the EM scattering by open-ended waveguide cavities," Ph.D. dissertation, The Ohio State University, Columbus, OH ,1989.
19. Kalbasi, K., and K. R. Demarest, "A multilevel enchancement of the method of moments", in *7th Ann. Rev. Progress Appl. Computat. Electromagn., Naval*, Monterey, CA, Mar. 1991, 254–263.
20. Lin, J. H., and W. C. Chew, "An application of nested equivalence principle algorithm (NEPAL) in matrix vector multiplication of iterative algorithm", *IEEE Antennas Propagat. Soc. Int. Symp. URSI Radio Sci. Meet.*, p. 317, Ann Arbor, MI, June 28–July 2, 1993.
21. Chew, W. C., and C. C. Lu, "The use of Huygen's equivalence principle for solving the volume integral equation of scattering", *IEEE Trans. Antennas Propagat.*, Vol. AP-41, No. 6, 897–904, July 1993.
22. Michielssen, E., and A. Boag, "Reduced representations of matrices generated by the method of moments," in *IEEE Int. Conf.* AP-S, 420–423, Seattle, WA, 1994.
23. Michielssen, E., and A. Boag, "Multilevel evaluation of electromagnetic fields for the rapid solution of scattering problems", *Microwave Opt. Technol. Lett.*, Vol. 7, 790–795. Dec. 1994.
24. Michielssen, E., and A. Boag, "A multilevel matrix decomposition algorithm for analyzing scattering from large structures", *IEEE Trans. Antennas Propagat.*, Vol. AP-44, No. 8, 1086–1093, Aug. 1996.
25. Beylkin, G., R. Coifman, and V. Rokhlin, "Fast wavelet transform and numerical algorthms I," *Comm. Pure Appl. Math.,* Vol. 44, 141–183, 1991.
26. Alpert, B. K., G. Beylkin, R. Coifman, and V. Rokhlin, "Wavelet-like bases for the fast solution of second-kind integral equations," *SIAM J. Sci. Comp.*, Vol. 14, 159–184, Jan. 1993.
27. Steinbery, B. Z., and Y. Leviatan, "On the use of wavelet expansions in method of moments," *IEEE Trans. Antennas Propagat.*, Vol. AP-41, No. 5, 610–619, May 1993.
28. Steinbery, B. Z., and Y. Leviatan, "Periodic wavelet expansions for analysis of scattering from metallic cylinders," *IEEE Antennas Propagat. Soc. Symp.*, 20–23, June 1994.
29. Wagner, R. L., P. Otto, and W. C. Chew, "Fast waveguide mode compuation using wavelet-like basis functions," *IEEE Microwave Guided Wave Lett.*, Vol. 3, 208–210, July 1993.

30. Franza, O. P., R. L. Wagner, and W. C. Chew, "Wavelet-like basis functions for solving scattering integral equation," *IEEE Antennas Propagat. Soc. Symp.*, 3–6, June 1994.
31. Kim, H., and H. Ling, "On the application of fast wavelet transform to the integral equation of electromagnetic scattering problems," *Microwave Opt. Technol. Lett.*, Vol. 6, No. 3, 168–173, Mar. 1993.
32. Goswami, J. C., A. K. Chan, and C. K. Chui, "On solving first-kind integral equations using wavelets on a bounded interval," *IEEE Trans. Antenna Propagat.*, Vol. AP-43, No. 6, 614–622, June 1995.
33. Wang, G., "A hybrid wavelet expansion and boundary element analysis of electromagnetic scattering from conducting objects," *IEEE Trans. Antenna Propagat.*, Vol. AP-43, No. 2, 170–178, Feb. 1995.